HHS Public Access

Author manuscript

Kidney Int. Author manuscript; available in PMC 2014 January 01.

Published in final edited form as:

Kidney Int. 2013 July ; 84(1): 130–137. doi:10.1038/ki.2013.63.

Uromodulin Upregulates TRPV5 by Impairing Caveolin-Mediated Endocytosis

Matthias T.F. Wolf[1], **Xue-Ru Wu**[2], and **Chou-Long Huang**[3]

[1]Department of Pediatrics, Division of Pediatric Nephrology, University of Texas Southwestern Medical Center, Dallas, TX 75390-9063, USA

[2]Departments of Urology and Pathology, New York University School of Medicine, New York, NY 10010, USA

[3]Department of Medicine, Division of Nephrology, University of Texas Southwestern Medical Center, Dallas. Texas 75390-8856, USA

Abstract

Uromodulin (UMOD) is synthesized in the thick ascending limb and secreted into urine as the most abundant protein. Association studies in humans suggest protective effects of UMOD against calcium-containing kidney stones. Mice carrying mutations of *Umod* found in human uromodulin-associated kidney disease (UAKD) and *Umod* deficient mice exhibit hypercalciuria. The mechanism for UMOD regulation of urinary Ca^{2+} excretion is incompletely understood. We examined if UMOD regulates TRPV5 and TRPV6, channels critical for renal transcellular Ca^{2+} reabsorption. Coexpression with UMOD increased whole-cell TRPV5 current density in HEK293 cells. In biotinylation studies UMOD increased TRPV5 cell-surface abundance. Extracellular application of purified UMOD upregulated TRPV5 current density within physiological relevant concentration ranges. UMOD exerted a similar effect on TRPV6. TRPV5 undergoes constitutive caveolin-mediated endocytosis. UMOD had no effect on TRPV5 in a caveolin-1 deficient cell line. Expression of recombinant caveolin-1 in these cells restored the ability of UMOD to upregulate TRPV5. Secretion of UAKD-mutant UMOD was markedly reduced and coexpression of mutant UMOD with TRPV5 failed to increase its current. Immunofluorescent studies demonstrated lower TRPV5 expression in $Umod^{-/-}$ mice compared to wild-type. UMOD upregulates TRPV5 by acting from extracellular and by decreasing endocytosis of TRPV5. The stimulation of Ca^{2+} reabsorption via TRPV5 by UMOD may contribute to protection against kidney stone formation.

Corresponding address: Matthias TF Wolf, MD, Division of Pediatric Nephrology, University of Texas Southwestern Medical Center, 5323 Harry Hines Blvd, Dallas, 75390-9063, TX, USA. Phone: +1-214-648-3438 / Fax: +1-214-648-2034; matthias.wolf@utsouthwestern.edu.

DISCLOSURES

None.

INTRODUCTION

Uromodulin (UMOD), also known as Tamm Horsfall protein, is the most abundant protein in normal human urine.[1,2] It is predominantly synthesized in the thick ascending limb (TAL) of Henle's loop as a membrane-bound glycosylphosphatidylinositol (GPI)-anchored protein and secreted into the urine after proteolytic cleavage of the C-terminus.[3,4] Mutations in *UMOD* were found to result in a variety of tubulointerstitial nephropathies including familial juvenile hyperuricemia (FJHN, OMIM #162000), medullary cystic kidney disease type II (MDCK2, OMIM #603860) and glomerulocystic kidney disease (GCKD, OMIM #609886).[5–8] These disorders, collectively termed uromodulin-associated kidney disease (UAKD), are characterized by hyperuricemia, hypertension, renal fibrosis, progressive renal failure and cyst formation.[5–8] *UMOD* mutations in UAKD result in impaired UMOD trafficking with accumulation of mutant proteins in the endoplasmatic reticulum (ER) leading to apoptosis of TAL cells.[9,10]

Although UMOD was discovered over 60 years ago, its physiological function remains poorly understood. Multiple lines of evidence suggest that UMOD may be involved in the regulation of renal tubular Ca^{2+} reabsorption. A genome wide association study in humans shows a protective effect of a specific *UMOD* allele against calcium-containing kidney stones.[11] It was reported that mice lacking *Umod* (also called Tamm-Horsfall knockout mice, herein referred to as *Umod*$^{-/-}$ mice) have hypercalciuria and spontaneous development of renal crystals.[12,13] Two different mouse models for human UAKD, one carrying the equivalent human C147W and another one carrying the A227T *UMOD* mutations, respectively, display hypercalciuria.[14,15] Whether UAKD patients have hypercalciuria before development of advanced tubulointerstitial renal disease has not been investigated.

Hypercalciuria is a strong risk factor for nephrolithiasis. Calcium is the predominant crystalline constituent of renal stones in 80% of cases.[16] Hypercalciuria is found in 35–50% of adult patients with nephrolithiasis.[17] Nephrolithiasis is a common disorder with a lifetime risk of 15–25% and results in significant distress, time loss from work, enormous health care cost, and in some instances loss of renal function.[16,18] Nephrolithiasis is thought to be caused by a sequence of events including urinary supersaturation, crystal nucleation, growth and finally adhesion.[18] Crystal nucleation can be prevented by small molecules like citrate and macromolecules such as UMOD and osteopontin.[18] It is believed that the anti-crystal effect of UMOD contributes to protection against kidney stone formation.[19,20] Regulation of urinary Ca^{2+} excretion by UMOD may also play an anti-nephrolithiasis role.

Renal Ca^{2+} excretion is important for the total body calcium homeostasis and thus closely regulated. In normal healthy adults, 95 to 98% of the filtered Ca^{2+} is reabsorbed by renal tubules.[17] The proximal tubule (PT) and TAL are responsible for the vast majority of Ca^{2+} reabsorption accounting for approximately 60% and 20%, respectively. In both segments Ca^{2+} reabsorption occurs via the paracellular pathway and is coupled to Na^{+} reabsorption.[17] The distal nephron including the late distal convoluted tubule (DCT) and connecting tubules (CNT) reabsorb approximately 10% of filtered Ca^{2+} load via the transcellular mechanism, which is the principal target for regulation of renal transcellular Ca^{2+} reabsorption by

hormones such as parathyroid hormone, vitamin D, and estrogen.[21] TRPV5 is a Ca^{2+}-selective channel expressed in the apical membrane of DCT and CNT which mediates Ca^{2+} entry from urine for transcellular reabsorption.[21] TRPV6 is a homolog of TRPV5 also present in the DCT and CNT and believed to form functional heteromultimers with TRPV5. [21] After entry through TRPV5/TRPV6, intracellular Ca^{2+} is bound to calbindin D_{28K} and exported from the cell at the basolateral side by the Na^{+}-Ca^{2+} exchanger NCX1 and Ca^{2+}-ATPase (PMCA1b).[21,22] Unlike Ca^{2+} reabsorption in PT and TAL, transcellular Ca^{2+} reabsorption in the distal nephron is independent of Na^{+} reabsorption. In both mutant *Umod* mouse models the degree of urinary Ca^{2+} loss exceeds the urinary sodium loss by far.[14,15] The dissociation of hypercalciuria from urinary sodium excretion in mutant *Umod* mice suggests that UMOD may play a role in regulating transcellular Ca^{2+} reabsorption in the late DCT and CNT. Here, we examine the hypothesis that UMOD regulates TRPV5 and TRPV6 channels.

RESULTS

UMOD Upregulates TRPV5 by Increasing TRPV5 Cell Surface Abundance

We first examined the regulation of TRPV5 by UMOD using whole-cell patch-clamp recording of human embryonic kidney (HEK) 293 cells co-expressing the channel with or without UMOD. Cells expressing TRPV5 exhibited the characteristic strongly inward-rectifying current (Figure 1A), which was not observed in untransfected cells (not shown). Coexpression with UMOD increased TRPV5 current density by ~85% (Figure 1, A and B). To determine whether UMOD increases TRPV5 cell surface abundance we performed surface biotinylation assays. Cell surface abundance of TRPV5 was much higher in cells cotransfected with UMOD compared to control (Figure 1C), indicating that UMOD upregulates TRPV5 current density at least partly by increasing abundance of the channel in the cell membrane. Addition of UMOD antibody to supernatant abrogated the effect of UMOD on TRPV5 upregulation (Figure 1D), further supporting that role of UMOD in this effect.

UMOD Upregulates TRPV5 from the Extracellular Side

The cellular expression of UMOD and TRPV5 in renal tubules is different. UMOD is expressed predominantly in the TAL and to a lesser extent in the early DCT whereas TRPV5 is mostly expressed in more distal segments including late DCT and CNT.[4,23] UMOD is secreted into urine after proteolytic cleavage of the C-terminus;[3] we therefore tested the hypothesis that UMOD is secreted into culture media and upregulates TRPV5 from the extracellular space. HEK293 cells expressing TRPV5 were incubated with supernatant of media harvested from separate groups of cells transfected with either UMOD or control vector. As shown, supernatant from UMOD-transfected cells, but not from control cells, increased TRPV5 current density (Figure 2A).

We determined the dose-response relationship for UMOD regulation of TRPV5 using commercially available purified UMOD. The half-maximal concentration (EC_{50}) of UMOD for activation of TRPV5 was estimated at approximately 100 ng/ml (Figure 2B). This EC_{50} value is ~5–10 fold lower than the estimated concentration of UMOD in the lumen of DCT.[2]

Biotinylation assay showed that extracellular application of purified UMOD enhanced cell surface abundance of TRPV5 (Figure 2C). Cell-surface biotinylated TRPV5 protein consists of glycosylated and underglycosylated forms, probably because TRPV5 exists as tetramer in the plasma membrane and glycosylation of subunits may be heterogeneous. Thus, physiological concentrations of UMOD can increase the activity and surface abundance of TRPV5 acting from the extracellular space.

UMOD Upregulates TRPV6

TRPV6 is another highly Ca^{2+} selective channel closely related to TRPV5.[24] It has a broader tissue distribution than TRPV5, is abundantly expressed in intestine and several other epithelial tissues besides kidney.[24] In the kidney, TRPV6 is expressed in the apical membrane of segments from DCT to medullary collecting duct, and may contribute to transcellular Ca^{2+} reabsorption by forming heteromultimers with TRPV5 in DCT and CNT or independently in collecting ducts.[25,26] We tested whether UMOD also regulates TRPV6. Cells expressing TRPV6 exhibited the characteristic inward-rectifying TRPV6 currents (Figure 3A, B), and extracellular application of purified UMOD increased TRPV6 current density in a concentration similar to that for TRPV5 (Figure 2B and 3C). EC_{50} for UMOD activation of TRPV6 was estimated at approximately 300 ng/ml (Figure 3C), which is slightly higher than that for TRPV5 but within the normal physiological concentration ranges of UMOD. Biotinylation assay showed that extracellular application of purified UMOD enhanced cell surface abundance of TRPV6 (Figure 3D).

UMOD Upreguates TRPV5 by Impairing Caveolin-Mediated Endocytosis

The increase in the steady-state cell-surface protein abundance may be caused by increased synthesis and insertion, decreased endocytosis or both. Increase in protein synthesis and insertion generally requires intracellular mechanisms. We therefore asked whether extracellular UMOD upregulates TRPV5 by affecting the dynamin- and caveolin-dependent constitutive endocytosis as previously described for TRPV5.[27,28] We examined the role of dynamin and caveolin, respectively, by blocking with dominant-negative mutant dynamin and using caveolin-1-deficient (*Cav1*$^{-/-}$) cell line. Though there are three major caveolin isoforms, caveolin-1 is an essential structural component of caveolae in all cell types except muscles.[29]

Our results revealed that incubation with purified UMOD increased TRPV5 current density cotransfected with wild-type dynamin II but not when cells were cotransfected with a dominant negative (K44A) dynamin II (Figure 4A). The finding that baseline TRPV5 current (i.e. without UMOD) in cells cotransfected with dominant-negative dynamin is relatively higher than that in cells cotransfected with wild type dynamin also supports the notion that TRPV5 is constitutively internalized. Stimulation of TRPV5 current density by UMOD was abrogated when channels were expressed in *Cav1*$^{-/-}$ cells but not when expressed in control cells (Figure 4B). Finally, forced expression of recombinant caveolin-1 (but not the control vector) in *Cav1*$^{-/-}$ cells restored the stimulation of TRPV5 by UMOD (Figure 4C). Collectively, these results support the conclusion that UMOD upregulates TRPV5 by decreasing endocytosis of channel proteins via dynamin- and caveolin-1-mediated pathways.

Reduced Secretion Underlies Decreased Stimulation of TRPV5 by Mutant UMOD

Mice carrying human UAKD *UMOD* mutations have hypercalciuria. We examined the effect of a *UMOD* mutation on the ability of TRPV5 stimulation. HEK293 cells were cotransfected with TRPV5 and with either wild-type UMOD or C150S UMOD corresponding to a human *UMOD* mutation. Cotransfection with C150S UMOD did not upregulate TRPV5 current density compared to wild-type UMOD (Figure 5A).

Human UAKD patients and mouse models of UAKD both have marked reduction in urinary excretion of UMOD.[14,30,31] Trafficking defects and retention in the ER are thought to be responsible for the decreased urinary secretion of mutant UMOD.[9] Impaired processing and secretion of mutant UMOD have also been described in a MDCK cell culture model.[9,32] We examined whether reduced mutant C150S UMOD secretion into cell culture media may account for the lack of stimulation of TRPV5 by mutant UMOD as observed above. HEK293 cells were transfected with wild-type or C150S UMOD and supernatant was harvested 36 hr or 60 hr later. Incubation with supernatant harvested from cells expressing wild type UMOD increased TRPV5 current by ~100%, but supernatant from cells expressing mutant UMOD for 36 hr did not cause a significant increase in TRPV5 current (Figure 5B). Supernatant harvested from cells expressing mutant UMOD after 60 hr stimulated TRPV5, but to a smaller extent compared to the wild-type supernatant. Thus, mutant UMOD is functionally active toward TRPV5 and the effect of the C150S *UMOD* mutation is likely due to impaired secretion into media.

The concentration of UMOD in the culture media is below detection by direct western blot analysis. We therefore compared the abundance of wild-type and mutant UMOD in the media after immunoprecipitation. Figure 5C is a representative gel showing that mutant C150S UMOD in the supernatant of culture media is significantly less abundant than wild-type UMOD. Results of multiple similar experiments are summarized in Figure 5D. Interestingly, while wild-type UMOD exists in glycosylated and un-glycosylated forms in supernatant and the total cell lysate, while mutant UMOD exists in a predominantly un-glycosylated protein in the total lysate (Figure 5C). This finding is consistent with the notion that mutant UMOD is not properly processed after protein synthesis and is retained in the ER.

Decreased TRPV5 expression in kidneys of *UMOD*$^{-/-}$ mice

To further support the physiological importance of the above pathway we analyzed the expression of TRPV5 in kidneys of wild-type and *Umod*$^{-/-}$ mice using immunofluorescent staining. Previously, *Umod*$^{-/-}$ mice (also known as Tamm-Horsfall knockout mice) were shown to have hypercalciuria.[13] Using an antibody previously used by other groups[33,34], we found that TRPV5 is expressed in the apical membrane of distal nephron of wild-type kidney (Figure 6). We have also confirmed the specificity of antibody by western-blot analysis (data not shown). Compared to wild-type mice, the expression of TRPV5 is markedly reduced in the *Umod*$^{-/-}$ mice.

DISCUSSION

Our data demonstrate a novel function of urinary UMOD in regulating renal Ca^{2+} reabsorption which have important implications to the protective role of UMOD against nephrolithiasis. Previously, two mechanisms have been proposed to explain the role of UMOD in protecting against nephrolithiasis. One relates to the macromolecular properties of UMOD in preventing crystallization.[18–20] The other relates to the fact that mice carrying *Umod* mutations have hypercalciuria.[14,15] In these mouse models, damage to TAL cells caused by accumulation of mutant proteins in the ER would be expected to impair Na^+ reabsorption, and thus Ca^{2+} reabsorption in this tubular segment.[17] Hypercalciuria observed in mutant *Umod* mice, however, greatly exceeds the magnitude of urinary Na^+ loss.[14,15] Along the same line, mice with homozygous deletion of *Umod* also develop hypercalciuria despite no apparent urinary Na^+ wasting.[12,13] UMOD is predominantly produced and released by TAL cells, and TRPV5 and TRPV6 channels are expressed in the downstream segments and critical for transcellular Ca^{2+} reabsorption. Our present finding that extracellular UMOD stimulates TRPV5 and TRPV6 channel activity provides an alternative mechanism for renal Ca^{2+} wasting independently of Na^+ wasting in conditions of decreased urinary concentration of UMOD. It should be cautioned that due to rarity of UAKD disease and tubulointerstitial damage occurring as part of the disease process, it remains unclear whether UAKD patients develop hypercalciuria before the onset of significant renal disease.

UMOD is the most abundant protein in human urine and multiple potential roles have been suggested for it. Besides prevention of calcium oxalate kidney stones,[12,13] UMOD is also reported to decrease the risk of urinary tract infections,[35] and is involved in myeloma and cast kidney formation.[36,37] It is also suggested that UMOD polymerizes to a gel-like structure which could be important for water impermeability of the TAL, thus contributing to regulation of water reabsorption.[38] With respect to ion transport, recent publications have suggested that UMOD regulates K^+ channel ROMK2 and Na^+-K^+-$2Cl^-$ cotransporter NKCC2 in the TAL.[39,40] ROMK2 and NKCC2 coexpress with UMOD in TAL and their regulation by UMOD occurs via intracellular mechanisms.[39,40] Our finding that UMOD secreted from TAL travels downstream to regulate TRPV5/6 in the distal nephron represents a new mode of action for UMOD. The estimated EC_{50} for UMOD activation of TRPV5/6 is significantly lower than the estimated concentration of UMOD in the lumen of DCT, suggesting that in most conditions TRPV5/6 channels are near-maximally active from the perspective of regulation by UMOD. This prediction is probably overzealous given that UMOD forms polymers as macromolecules and the effective concentration of macromolecular UMOD is probably much lower than that of UMOD monomer. Whether production and secretion of UMOD by TAL is regulated and conditions by which it may lead to altered Ca^{2+} reabsorption remain to be investigated.

The mechanism by which UMOD inhibits endocytosis of TRPV5/6 channels remains unknown. The fact that UMOD regulates TRPV5 expressed in multiple different cell lines (HEK293, Cav1-null and control thymus fibroblasts) suggests that the regulation does not involve renal-specific membrane receptors. Regulation of ion transporters on the luminal membrane by urinary proteins through a direct action on their extracellular domain is not unprecedented. Proteases such as prostasin, channel activating protease CAP1, and plasmin

cleave subunits of epithelial Na^+ channel ENaC to enhance its activity.[41–44] Soluble Klotho present in the urine also regulates sodium-phosphate cotransporter NaPi, ROMK, TRPV5 and TRPV6 from the luminal side.[28,45–47] The regulation of ROMK and TRPV5 by soluble Klotho involves enzymatic activity; cleavage of sialic acids in the N-glycan of these channels allows them to bind to galectin-1 at the extracellular surface. This binding leads to decreased endocytosis and increased abundance of channels at the cell surface.[28,47] It is intriguing to consider the possibility that UMOD forms a macromolecular structure at the cell surface of distal tubules (as is similarly suggested for TAL) and interacts with TRPV5/6 directly or indirectly through galectin-1 to regulate the kinetics of endocytosis of the channels.

In summary, we provide compelling data to suggest that UMOD is an important regulator of TRPV5/6-mediated renal Ca^{2+} reabsorption and this effect may contribute to the ability of UMOD to protect against kidney stone formation. These findings open new avenues for investigating renal Ca^{2+} handling in various physiological and pathological conditions.

CONCISE METHODS

Materials and DNA Constructs

Purified UMOD (from human urine) was purchased from SunnyLab (Sittingbourne, United Kingdom). The rabbit polyclonal anti-GFP-peroxidase antibody was obtained from Invitrogen/Molecular Probes (Eugene, OR). EZ-Link® Sulfo-NHS-SS-biotin and streptavidin-agarose beads were obtained from Thermo Scientific (Rockford, IL). Protein G immobilized on agarose, mouse monoclonal anti-HA antibody and mouse monoclonal anti-β-actin-peroxidase antibody were purchased from Sigma (Saint Louis, MO). Cappel antibody against human uromucoid (Tamm-Horsfall glycoprotein) from goat was purchased from MP Biochemicals (Solon, OH). Donkey antibody against goat IgG was obtained from Santa Cruz Biotechnology (Santa Cruz, CA). GFP-tagged TRPV5 contains the coding region of TRPV5 cloned in-frame to a commercial pEGFP-N3 vector.[28] cDNA for caveolin-1 is in a pcDNA3 vector.[27] Flag-tagged TRPV6 was provided by Dr. JB Peng.[48]

Cell Culture and Transfection

HEK293 cells were cultured as described.[27] Wild-type and caveolin-1 null ($Cav1^{-/-}$) fibroblasts were cultured in low glucose DMEM supplemented with 10% fetal bovine serum, glutamine, penicillin, and streptomycin. [27] Cells were transiently cotransfected with cDNA for wild-type GFP-TRPV5 (300 ng per 6-well) plus cDNA for wild-type UMOD, C150S mutant UMOD, caveolin-1, and/or wild-type or dominant-negative (K44A) rat dynamin II as indicated in each experiment. Transfection was performed using Polyfect® reagent (Qiagen, Valencia, CA) per manufacturer's protocol. In each experiment the total amount of DNA for transfection was balanced by using empty vectors.

Electrophysiological Recordings

Approximately 48 h after transfection cells were dissociated and placed in a chamber for ruptured whole-cell recordings as described previously.[27] Transfected cells were identified for recording by green fluorescence. The pipette and bath solution contained (in mM) 140

Na-Asp (sodium aspartate), 10 NaCl, 10 EDTA, and 10 HEPES (pH 7.4), and 140 Na-Asp, 10 NaCl, 1 EDTA, and 10 HEPES (pH 7.4), respectively. The resistance of electrodes containing the pipette solution was 1.5–3 MΩ. The cell membrane capacitance and series resistance were monitored and compensated (>75%) electronically using an Axopatch 200B amplifier (Axon Instruments, Foster City, CA). Voltage protocol consists of 0 mV holding potential and successive voltage sets (500-ms duration) from −150 to +100 mV in +25 increments. Data acquisition was performed using ClampX9.2 software (Axon Instruments). Currents were low-pass filtered at 2 kHz using 8-pole Bessels filter in the clamp amplifier, sampled every 0.1 ms (10kHz) with Digidata-1300 interface, and stored directly to a computer hard drive.

Surface Biotinylation Assay

For biotinylation of cell surface TRPV5, cells were washed with ice-cold PBS and incubated 0.75 ml PBS containing 0.75 mg/ml EZ-Link-NHS-SS-biotin for 1h at 4°C. After being quenched with glycine (100 mM), cells were lysed in RIPA buffer (150 mM NaCl, 50 mM Tris-HCl, 5 mM EDTA, 1% Triton X-100, 0.5% DOC, and 0.1% SDS) containing protease inhibitor cocktail (Roche, Indianapolis, IN). Biotinylated proteins were precipitated by streptavidin-agarose beads. Beads were subsequently washed four times with PBS containing 1% Triton X-100. Biotin-labeled proteins were eluted in sample buffer, heated at 50°C for 5 min and separated by SDS-PAGE electrophoresis, and transferred to nitrocellulose membranes for Western blotting. TRPV5 proteins on the membrane were detected using a rabbit polyclonal anti-GFP antibody. Biotinylation experiments were performed three times with similar results.

Immunoprecipitation Assay

Medium of HA-tagged wild-type or C150S mutant UMOD transfected HEK293 cells was harvested and diluted 1:1 with protease inhibitor cocktail containing PBS. Protein G agarose beads were washed three times in PBS. Harvested supernatant was pre-cleared by adding washed protein G beads for 1 h. Supernatant was removed and incubated over night with 5 μg of mouse monoclonal anti-HA antibody. Newly prepared protein G agarose beads were used for binding of the UMOD-anti-HA antibody complex for 2 h. Afterwards beads were washed three times in PBS, separated by SDS-PAGE electrophoresis, and transferred to nitrocellulose membranes for Western blotting. Wild-type and mutant UMOD were detected using goat antiserum to human uromucoid (Tamm-Horsfall glycoprotein) (MP Biochemicals).

Immunofluorescent staining

The *Umod*$^{-/-}$ mouse (also known as Tamm-Horsfall (THP) knockout mouse) has been previously described.[12,13,49] The knockout mouse was generated by targeted deletion of exons 1 to 4, which resulted in complete absence of *Umod* in kidneys of knockout mice. Male wild-type and *Umod*$^{-/-}$ mice were fed a regular diet and sacrificed at the age of 4 months. Mice were anesthetized with Avertin and perfused by cardiac puncture with 15 ml of PBS followed by 15 ml of 4% paraformaldehyde. The kidneys of wild-type and *Umod*$^{-/-}$ mice were harvested and embedded in paraffin. The sections were deparaffinized and

antigen retrieval with Trilogy (Cell Marque) for 18 minutes at 70 degree Celcius was performed. Endogenous peroxidase activity was blocked by incubation with 0.3% H_2O_2. Sections were blocked for 1 h with 10% donkey sera in PBS. Sections were stained with 1:50 rabbit anti-rat ECaC1 (TRPV5) antibody (Alpha Diagnostic International, San Antonio, TX) overnight. This was followed by PBS washes and incubation with secondary antibody Alexa Fluor donkey anti-rabbit IgG 555 (1:200) for 2 hours. Negative controls were obtained only using the secondary antibody. The fluorescent and DIC Nomarski images were obtained using a Zeiss Axioplan 2 microscope (Zeiss, Jena, Germany) with a Zeiss AxioCam MRc camera (Zeiss, Jena, Germany). All animal experiments were performed in compliance with relevant laws and institutional guidelines and were approved by the University of Texas Southwestern Medical Center at Dallas Institutional Animal Care and Use Committee.

Data Analysis

Data analysis and curve fitting were performed with the Prism (v3.0) software (GraphPad Software, San Diego, CA). Statistical comparison between two groups of data was made using two-tailed unpaired *t*-test. Data are presented as means ± SEM (n = 5–10 as indicated).

Acknowledgments

We thank Dr. Luca Rampoldi for wild-type and C150S mutant UMOD constructs, Dr. Ji-Bin Peng for TRPV6 construct, and Drs. Michel Baum and Orson Moe for discussions and comments. We are very grateful to Zhufeng Yang and Denise Marciano for assistance with perfusion and immunofluorescent staining. The study was supported by grants from National Institutes of Health (RO1-DK85726, K08-DK095994-01, K12-HD000850, T32DK007257-28 grant). Matthias T.F. Wolf was a Fellow of the Pediatric Scientist Development Program. CLH holds the Jacob Lemann Professorship in Calcium Transport of University of Texas Southwestern Medical Center.

References

1. Tamm I, Horsfall FL Jr. Characterization and separation of an inhibitor of viral hemagglutination present in urine. Proc Soc Exp Biol Med. 1950; 74:106–108. [PubMed: 15430405]
2. Pennica D, Kohr WJ, Kuang WJ, et al. Identification of human uromodulin as the Tamm-Horsfall urinary glycoprotein. Science. 1987; 236:83–88. [PubMed: 3453112]
3. Santambrogio S, Cattaneo A, Bernascone I, et al. Urinary uromodulin carries an intact ZP domain generated by a conserved C-terminal proteolytic cleavage. Biochem Biophys Res Commun. 2008; 370:410–413. [PubMed: 18375198]
4. Bachmann S, Metzger R, Bunnemann B. Tamm-Horsfall protein-mRNA synthesis is localized to the thick ascending limb of Henle's loop in rat kidney. Histochemistry 1990. 1990; 94:517–523.
5. Hart TC, Gorry MC, Hart PS, et al. Mutations of the *UMOD* gene are responsible for medullary cystic kidney disease 2 and familial juvenile hyperuricaemic nephropathy. J Med Genet. 2002; 39:882–892. [PubMed: 12471200]
6. Dahan K, Devuyst O, Smaers M, et al. A cluster of mutations in the *UMOD* gene causes familial juvenile hyperuricemic nephropathy with abnormal expression of *Uromodulin*. J Am Soc Nephrol. 2003; 14:2883–2893. [PubMed: 14569098]
7. Rampoldi L, Caridi G, Santon D, et al. Allelism of MCKD, FJHN, and GCKD caused by impairment of uromodulin export dynamics. Hum Mol Genet. 2003; 12:3369–3384. [PubMed: 14570709]
8. Wolf MT, Mucha BE, Attanasio M, et al. Mutations of the *Uromodulin* gene in MCKD type 2 patients cluster in exon 4 which encodes three EGF-like domains. Kidney Int. 2003; 64:1580–1587. [PubMed: 14531790]

9. Bernascone I, Vavassori S, Di Pentima A, et al. Defective intracellular trafficking of uromodulin mutant isoforms. Traffic. 2006; 7:1567–1579. [PubMed: 17010121]
10. Choi SW, Ryu OH, Choi SJ, et al. Mutant tamm-horsfall glycoprotein accumulation in endoplasmic reticulum induces apoptosis reversed by colchicine and sodium 4-phenylbutyrate. J Am Soc Nephro. 2005; 16:3006–3014.
11. Gudbjartsson DF, Holm H, Indridason OS, et al. Association of variants at UMOD with chronic kidney disease and kidney stones-role of age and comorbid diseases. PLoS Genet. 2010; 6:e1001039. [PubMed: 20686651]
12. Mo L, Huang HY, Zhu XH, et al. Tamm-Horsfall protein is a critical renal defense factor protecting against calcium oxalate crystal formation. Kidney Int. 2004; 66:1159–1166. [PubMed: 15327412]
13. Liu Y, Mo L, Goldfarb DS, et al. Progressive renal papillary calcification and ureteral stone formation in mice deficient for Tamm-Horsfall protein. Am J Physiol Renal Physiol. 2010; 299:F469–478. [PubMed: 20591941]
14. Kemter E, Rathkolb B, Rozman J, et al. Novel Missense Mutation of Uromodulin in Mice Causes Renal Dysfunction with Alterations in Urea Handling, Energy and Bone Metabolism. Am J Physiol Renal Physiol. 2009; 297:F1391–1398. [PubMed: 19692485]
15. Bernascone I, Janas S, Ikehata M, et al. A transgenic mouse model for uromodulin-associated kidney diseases shows specific tubulo-interstitial damage, urinary concentrating defect and renal failure. Hum Mol Genet. 2010; 19:2998–3010. [PubMed: 20472742]
16. Moe OW, Pearle MS, Sakhaee K. Pharmacotherapy of urolithiasis: evidence from clinical trials. Kidney Int. 2011; 79:385–392. [PubMed: 20927039]
17. Frick KK, Bushinsky DA. Molecular mechanisms of primary hypercalciuria. J Am Soc Nephrol. 2003; 14:1082–1095. [PubMed: 12660344]
18. Kumar V, Lieske JC. Protein regulation of intrarenal crystallization. Curr Opin Nephrol Hypertens. 2006; 15:374–380. [PubMed: 16775451]
19. Kumar V, Peña de la Vega L, Farell G, Lieske JC. Urinary macromolecular inhibition of crystal adhesion to renal epithelial cells is impaired in male stone formers. Kidney Int. 2005; 68:1784–1792. [PubMed: 16164655]
20. Hess B, Nakagawa Y, Coe FL. Inhibition of calcium oxalate monohydrate crystal aggregation by urine proteins. Am J Physiol. 1989; 257:F99–106. [PubMed: 2750929]
21. Hoenderop JG, Bindels RJ. Calciotropic and magnesiotropic TRP channels. Physiology. 2008; 23:32–40. [PubMed: 18268363]
22. Koster HP, Hartog A, Van Os CH, Bindels RJ. Calbindin-D28K facilitates cytosolic calcium diffusion without interfering with calcium signaling. Cell Calcium. 1995; 18:187–196. [PubMed: 8529259]
23. Hoenderop JG, Hartog A, Stuiver M, et al. Localization of the epithelial Ca(2+) channel in rabbit kidney and intestine. J Am Soc Nephrol. 2000; 11:1171–1178. [PubMed: 10864572]
24. Peng JB, Chen XZ, Berger UV, et al. Molecular cloning and characterization of a channel-like transporter mediating intestinal calcium absorption. J Biol Chem. 1999; 274:22739–22746. [PubMed: 10428857]
25. Chang Q, Gyftogianni E, van de Graaf SF, et al. Molecular determinants in TRPV5 channel assembly. J Biol Chem. 2004; 279:54304–54311. [PubMed: 15489237]
26. Nijenhuis T, Hoenderop JG, van der Kemp AW, Bindels RJ. Localization and regulation of the epithelial Ca2+ channel TRPV6 in the kidney. J Am Soc Nephrol. 2003; 14:2731–2740. [PubMed: 14569082]
27. Cha SK, Wu T, Huang CL. Protein kinase C inhibits caveolae-mediated endocytosis of TRPV5. Am J Physiol Renal Physiol. 2008; 294:F1212–1221. [PubMed: 18305097]
28. Cha SK, Ortega B, Kurosu H, et al. Removal of sialic acid involving Klotho causes cell-surface retention of TRPV5 channel via binding to galectin-1. Proc Natl Acad Sci U S A. 2008; 105:9805–9810. [PubMed: 18606998]
29. Parton RG, Simons K. The multiple faces of caveolae. Nat Rev Mol Cell Biol. 2007; 8:185–194. [PubMed: 17318224]

30. Bleyer AJ, Hart TC, Shihabi Z, et al. Mutations in the uromodulin gene decrease urinary excretion of Tamm-Horsfall protein. Kidney Int. 2004; 66:974–977. [PubMed: 15327389]
31. Wolf MTF, Beck BB, Misselwitz J, et al. The *Uromodulin* C744G mutation causes MCKD2 and FJHN in children and adults and may be due to a possible founder effect. Kidney Int. 2007; 71:574–581. [PubMed: 17245395]
32. Schaeffer C, Cattaneo A, Trudu M, et al. Urinary secretion and extracellular aggregation of mutant uromodulin isoforms. Kidney Int. 2012; 81:769–778. [PubMed: 22237754]
33. Lee CT, Shang S, Lai LW, et al. Effect of thiazide on renal gene expression of apical calcium channels and calbindins. Am J Physiol Renal Physiol. 2004; 287:F1164–1170. [PubMed: 15265769]
34. Lee CT, Chen HC, Lai LW, et al. Effects of furosemide on renal calcium handling. Am J Physiol Renal Physiol. 2007; 293:F1231–1237. [PubMed: 17652376]
35. Bates JM, Raffi HM, Prasadan K, et al. Tamm-Horsfall protein knockout mice are more prone to urinary tract infection: rapid communication. Kidney Int. 2004; 65:791–797. [PubMed: 14871399]
36. Rhodes DCJ. Binding of Tamm-Horsfall protein to complement 1q and complement 1, including influence of hydrogen-ion concentration. Immunol Cell Biol. 2002; 78:558–566. [PubMed: 12406390]
37. Ying WZ, Sanders PW. Mapping the binding domain of immunoglobulin light chains for Tamm-Horsfall protein. Am J Pathol. 2001; 158:1859–1866. [PubMed: 11337384]
38. Wiggins RC. Uromucoid (Tamm-Horsfall glycoprotein) forms different polymeric arrangements on a filter surface under different physicochemical conditions. Clin Chim Acta. 1987; 162:329–340. [PubMed: 3568408]
39. Mutig K, Kahl T, Saritas T, et al. Activation of the bumetanide-sensitive Na+,K+,2Cl−-cotransporter NKCC2 is facilitated by Tamm-Horsfall protein in a chloride-sensitive manner. J Biol Chem. 2011; 286:30200–30210. [PubMed: 21737451]
40. Renigunta A, Renigunta V, Saritas T, et al. Tamm-Horsfall glycoprotein interacts with renal outer medullary potassium channel ROMK2 and regulates its function. J Biol Chem. 2011; 286:2224–2235. [PubMed: 21081491]
41. Vallet V, Chraibi A, Gaeggeler HP, et al. An epithelial serine protease activates the amiloride-sensitive sodium channel. Nature. 1997; 389:607–610. [PubMed: 9335501]
42. Bruns JB, Carattino MD, Sheng S, et al. Epithelial Na+ channels are fully activated by furin- and prostasin-dependent release of an inhibitory peptide from the gamma-subunit. J Biol Chem. 2007; 282:6153–6160. [PubMed: 17199078]
43. Passero CJ, Mueller GM, Rondon-Berrios H, et al. Plasmin activates epithelial Na+ channels by cleaving the gamma subunit. J Biol Chem. 2008; 283:36586–36591. [PubMed: 18981180]
44. Svenningsen P, Bistrup C, Friis UG, et al. Plasmin in nephrotic urine activates the epithelial sodium channel. J Am Soc Nephrol. 2009; 20:299–310. [PubMed: 19073825]
45. Chang Q, Hoefs S, van der Kemp AW, et al. The beta-glucuronidase klotho hydrolyzes and activates the TRPV5 channel. Science. 2005; 310:490–493. [PubMed: 16239475]
46. Hu MC, Shi M, Zhang J, et al. Klotho: a novel phosphaturic substance acting as an autocrine enzyme in the renal proximal tubule. FASEB J. 2010; 24:3438–3450. [PubMed: 20466874]
47. Cha SK, Hu MC, Kurosu H, et al. Regulation of renal outer medullary potassium channel and renal K(+) excretion by Klotho. Mol Pharmacol. 2009; 76:38–46. [PubMed: 19349416]
48. Zhang W, Na T, Wu G, et al. Down-regulation of intestinal apical calcium entry channel TRPV6 by ubiquitin E3 ligase Nedd4-2. J Biol Chem. 2010; 285:36586–36596. [PubMed: 20843805]
49. Mo L, Zhu XH, Huang HY, et al. Ablation of the Tamm-Horsfall protein gene increases susceptibility of mice to bladder colonization by type 1-fimbriated Escherichia coli. Am J Physiol Renal Physiol. 2004; 286:F795–802. [PubMed: 14665435]

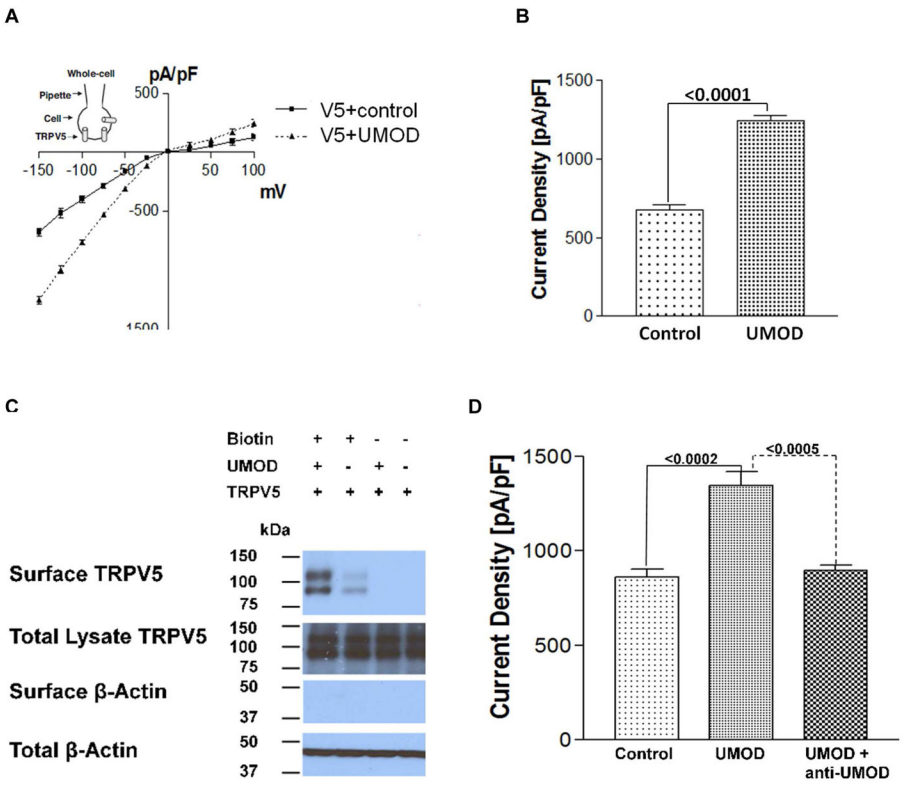

Figure 1.

UMOD increases TRPV5 current density and cell surface abundance. (A) Coexpression of UMOD and TRPV5 results in increasing TRPV5 current density. HEK293 cells were cotransfected with GFP-tagged wild-type TRPV5 and with or without ***UMOD*** for 48 hr. TRPV5 current density (current normalized to cell surface area; pA/pF; mean ± SEM) was evoked by test pulses from −150 to +100 mV with +25 mV increments for 500 ms and steady-state current-voltage (I–V) relation curve showed typical inwardly rectifying TRPV5 currents in cells cotransfected with TRPV5 and ***UMOD*** vs. control (***n*** = 5 for each). (B) Bar graph shows TRPV5 current density (pA/pF) at −150 mV cotransfected with ***UMOD*** or without (Control). (C) Effect of UMOD on TRPV5 cell surface abundance measured by biotinylation assay. TRPV5 abundance at plasma membrane (top) and total lysates (middle) were analyzed by immunoblot analysis using antibody against GFP. The antibody did not detect protein signal in untransfected cells (not shown). The double bands of TRPV5 reflect un-glycosylated and glycosylated protein products. For detection of TRPV5 in the surface and lysate, 200 μg and 10 μg protein were separated by SDS gel electrophoresis, respectively. (D) Effect of anti-UMOD antibody on UMOD regulation of TRPV5. Anti-UMOD antibody was added to culture media of cells transfected with TRPV5 and with or without UMOD co-transfection.

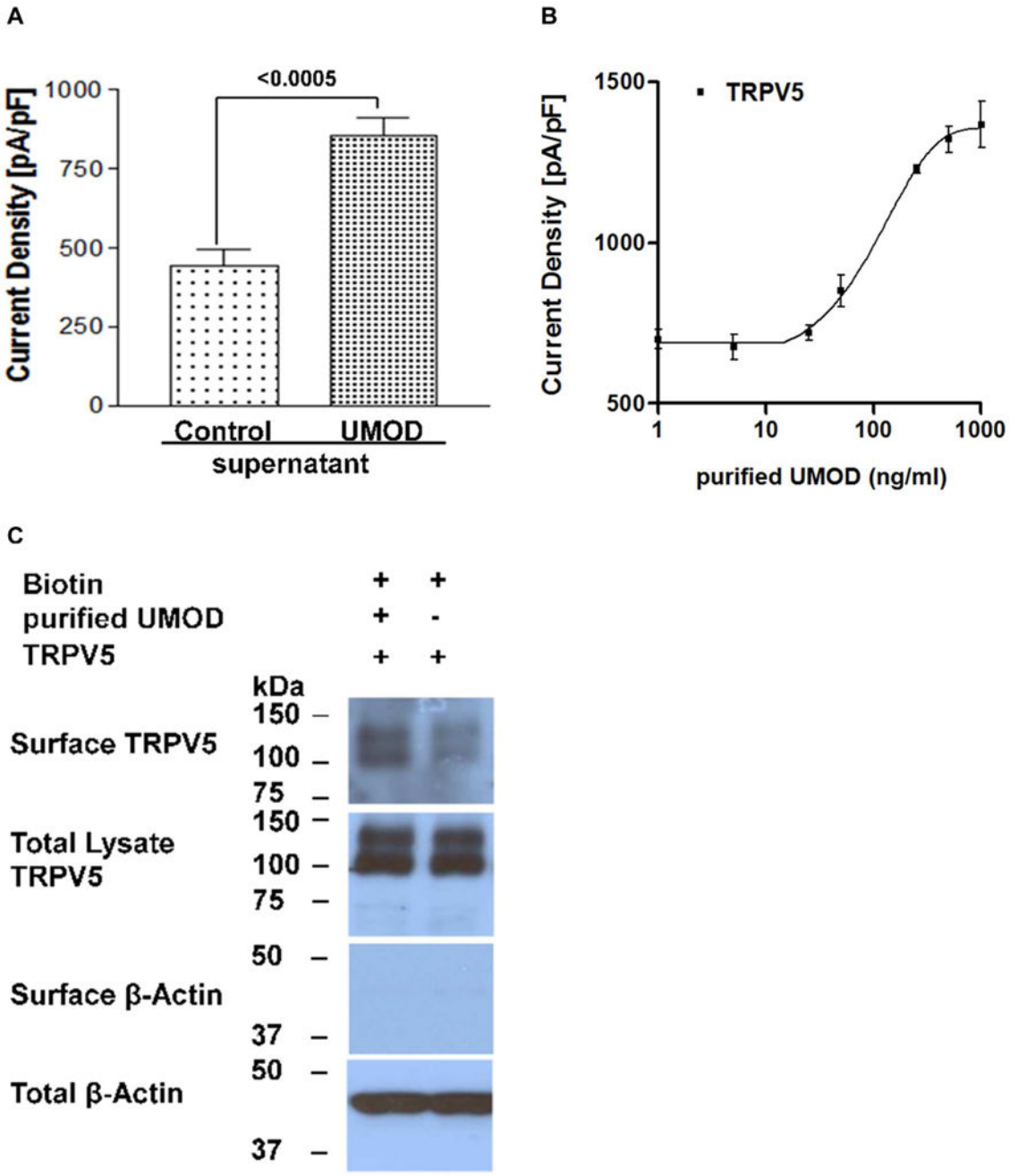

Figure 2.

UMOD upregulates TRPV5 from the extracellular side. (A) HEK293 cells were transfected with wild-type ***UMOD*** or control vector. Forty hours later, the control- and UMOD-containing supernatant was harvested to replace for media of separately cultured cells transfected with TRPV5. After replacement of media, TRPV5 expressing cells were further cultured overnight. Bar graph shows current density at −150 mV (***n*** = 5 for each). (B) Effect of increasing concentrations of purified UMOD (final concentration in the media) on TRPV5 current density. TRPV5 transfected cells were treated with purified UMOD overnight. (C) Effect of purified UMOD on TRPV5 cell surface abundance. Thirty-six hr

after transfection, TRPV5-expressing cells were treated with or without purified UMOD (1 μg/ml) overnight. TRPV5 abundance at plasma membrane (top) and total lysate (middle) were measured by immunoblot analysis using antibody against GFP.

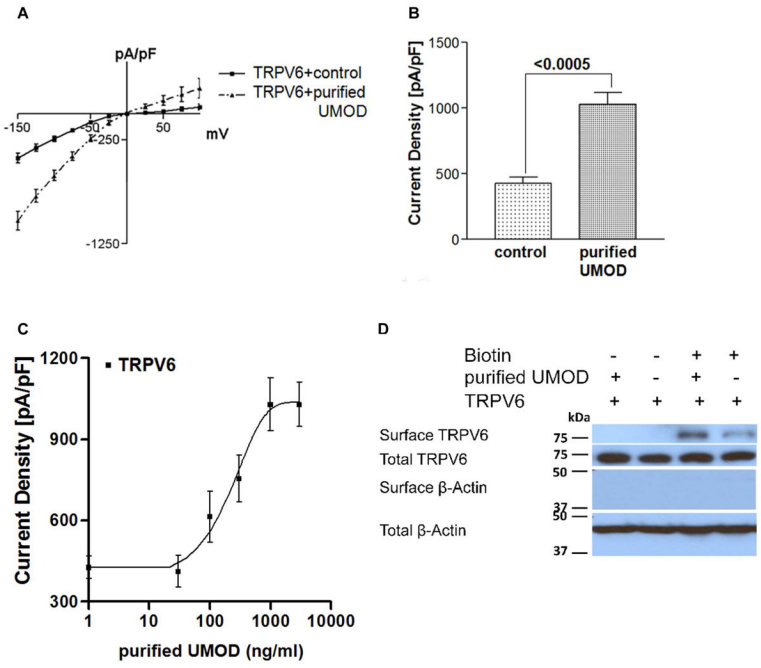

Figure 3.

UMOD upregulates TRPV6. (A) TRPV6-expressing cells were treated with or without purified UMOD (1 μg/ml) overnight. (B) Bar graph shows mean ± SEM (***n*** = 7 each) of TRPV6 current density at −150 mV. (C) Dose-dependent effect of purified UMOD on TRPV6. (D) Cell surface abundance of Flag-tagged TRPV6 with or without extracellular application of purified UMOD. TRPV6 abundance at plasma membrane (top) and total lysates (middle) were analyzed by immunoblot analysis using anti-Flag antibody.

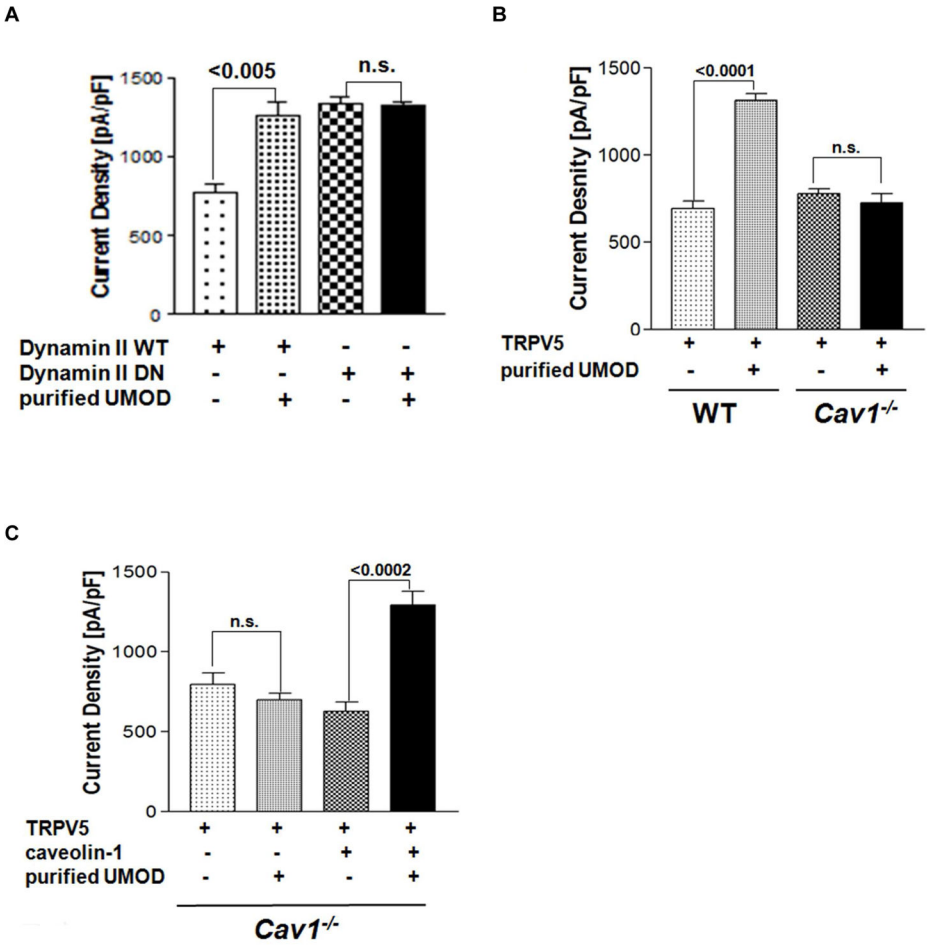

Figure 4.

UMOD upregulates TRPV5 by impairing dynamin- and caveolin-1 dependent endocytosis. (A) Cells were cotransfected with TRPV5 and with either wild-type or dominant-negative (K44A) dynamin II, and treated with purified UMOD (1 μg/ml) (***n*** = 6 for each). (B) Caveolin-1 (***Cav1***$^{-/-}$) null fibroblasts or control fibroblasts from thymus were transfected with TRPV5, and treated with purified UMOD (***n*** = 5 for each). (C) Caveolin-1 null (***Cav1***$^{-/-}$) cells were cotransfected with TRPV5 and with caveolin-1-expressing plasmid or empty vector, and treated with purified UMOD (***n***=5 for each).

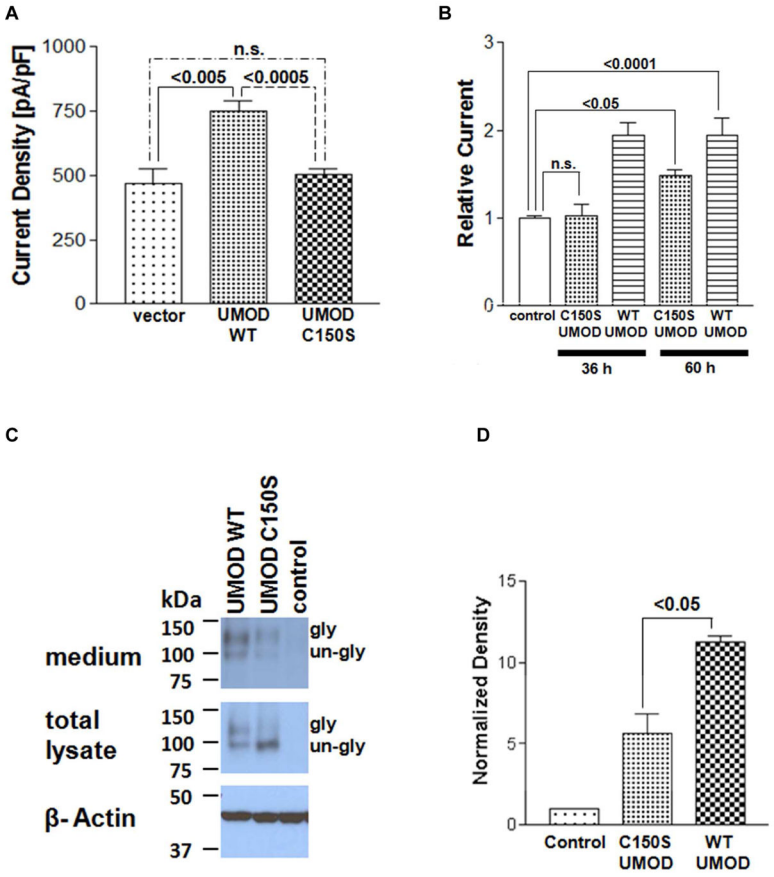

Figure 5.

Effect of C150S ***UMOD*** mutation on UMOD secretion and the ability to regulate TRPV5. (A) Cells were cotransfected with TRPV5 and with empty vector, wild-type ***UMOD*** or C150S (cysteine-150 to serine) mutant ***UMOD***, and recorded for TRPV5 currents. Bar graph shows current density at −150 mV (***n*** = 6 for each). (B) Supernatant was harvested from cells transfected with wild-type or C150S mutant ***UMOD*** for 36 hr or 60 hr to replace for media of separate cultured cells transfected with TRPV5. After replacement of media, TRPV5 expressing cells were further cultured overnight. Control indicates TRPV5-expressing without exposure to supernatant of wild-type or mutant UMOD. Data were mean ± SEM, ***n*** = 6 for each. (C) Top gel shows supernatant harvested from cells 36 hr after transfection expressing HA-tagged wild-type, mutant C150S UMOD or neither (control) after immunoprecipitation by anti-HA antibody and analyzed by western blotting. Middle gel is western blot analysis of total cell lysate from each of above conditions. Bottom gel is β-actin loading control. “gly” and “un-gly” indicate glycosylated and un-glycosylated UMOD protein, respectively. (D) Averaged results (mean ± SEM) from three experiments as shown in panel C. Abundance of UMOD protein (both glycosylated and un-glycosylated) immunoprecipitated from supernatant was quantified by densitometry (area under the curve). Density of protein abundance was normalized to that in the control vector group (given value 1).

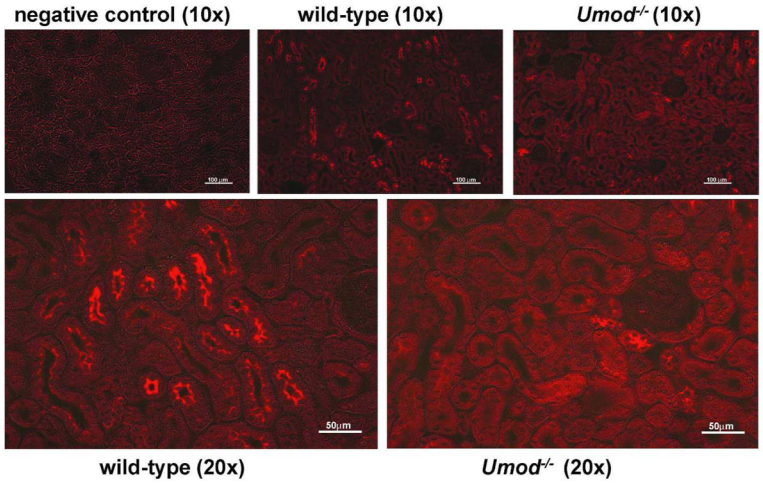

Figure 6.

Immunofluorescent staining of TRPV5 in wild-type and ***Umod***$^{-/-}$ mice. Immunofluorescent staining of TRPV5 (shown in red) in renal cortex of ***Umod***$^{-/-}$ mice (left upper and lower panel) is lower compared to wild-type mice (middle upper panel, left lower panel). Fluorescent images were overlapped with differential interference contrast images to better illustrate subcellular distribution. Shown are microscopic images obtained with x10 and x20 objective lenses. Scale bar in the upper panel represents 100 μm and 50μm in the lower panel. Negative control was obtained under identical experimental conditions as study sections except using primary antibody.